THE ASTROPHYSICAL JOURNAL, 267:837–843, 1983 April 15

SOLAR TYPE II RADIO EMISSION AND THE SHOCK DRIFT ACCELERATION OF ELECTRONS

GORDON D. HOLMAN
Astronomy Program, University of Maryland
AND
M. E. PESSES[1]
Solar Activity Branch, Laboratory for Astronomy and Solar Physics, NASA Goddard Space Flight Center
Received 1982 May 27; accepted 1982 October 7

ABSTRACT

Many of the properties of energetic electrons and ions accelerated by interplanetary shock waves can be understood in terms of the shock drift acceleration mechanism. In this paper we show that the shock drift acceleration of electrons can be responsible for solar type II radio bursts as well. We review the shock drift acceleration mechanism and show that the streaming distribution of reflected electrons produced upstream of the shock front by this mechanism can be unstable to the generation of electrostatic plasma waves, which in turn interact to produce the observed radio emission. We derive constraints upon the density and energy of suprathermal electrons required to produce a typical type II burst.

The production of type II emission by shock drift accelerated electrons requires that the shock normal be at a high angle (ψ) to the upstream magnetic field. For a 1000 km s^{-1} shock in a 2×10^6 K corona, a value of $\psi \gtrsim 80°$ is required. Reflected electrons are not obtained, however, when ψ is within a few degrees of 90°. We argue that these requirements are consistent with observations and show that a curved shock front propagating across magnetic field lines can naturally result in herringbone structure, herringbone structure without a backbone, or band splitting, the result depending upon the orientation and radius of curvature of the shock front and magnetic field lines and upon the energy of the accelerated electrons. We interpret the occurrence of band splitting and backboneless herringbone structure to the lack of reflected particles when ψ is near 90°. The electrons responsible for each band originate from different regions of the shock front, and, therefore, the emission from each band is predicted to arise from a differential spatial location. Particles transmitted downstream of the shock may contribute to moving type IV radio emission.

Subject headings: hydromagnetics — particle acceleration — shock waves — Sun: corona — Sun: radio radiation

I. INTRODUCTION

The frequency versus time plot of the radio flux (dynamic spectrum) of a typical solar type II radio burst is characterized by one or two parallel bands of emission which decrease in frequency with time (see Kundu 1965 and McLean 1974 for reviews). When both bands are present, the frequency ratio between the bands is approximately two, and they are understood to be radiation at the local electron plasma frequency, ω_e, and its second harmonic. The emission is apparently associated with a magnetohydrodynamic (MHD) shock wave propagating away from the site of a flare. The decrease in emission frequency with time results from the decreasing plasma density ($\propto \omega_e^2$) as the shock propagates outward through the corona.

The production of the radio emission requires the generation of an enhanced level of electrostatic plasma waves (with $\omega \approx \omega_e$) in the vicinity of the shock wave (cf. Melrose 1980). These waves can then interact with ion density fluctuations or ion sound waves to produce radio emission at the plasma frequency, and with each other to produce emission at the second harmonic. The growth of these waves is most likely induced by a population of suprathermal streaming electrons which is associated with the shock wave (see Klinkhamer and Kuijpers, 1981, however, for an alternative possibility). An understanding of how and precisely where these suprathermal electrons are produced has been elusive, however, because of an insufficient knowledge of MHD shock structure and our inability to obtain *in situ* measurements of coronal shock waves. On the other hand, suprathermal protons are directly observed to be accelerated by interplanetary shock waves (see Pesses, Decker,

[1]NAS/NRC Resident Research Associate.

and Armstrong 1982 for a review and additional references). More recently, *in situ* observations of suprathermal electrons accelerated by interplanetary shock waves have been obtained (Potter 1981). The purpose of this paper is to make use of these observations and related theoretical work to develop a model for the production of type II radio emission by coronal shock waves.

The generation of type II emission by an MHD shock is a three-step process: (1) a distribution of streaming suprathermal electrons is produced in the vicinity of the shock wave; (2) this distribution stimulates the growth of electrostatic plasma waves; and (3) these waves then interact with the ambient plasma and themselves to produce the observed radio emission. Many of the properties of the particles observed in interplanetary shocks can be understood as the shock drift acceleration of charged particles in the plane of an oblique, fast-mode MHD shock wave. In this paper we show that the shock drift acceleration of electrons can be responsible for type II radio bursts as well. In § II we review shock drift acceleration and the relevant observations of particle acceleration in interplanetary shock waves. In § III we determine the conditions which are required for the generation of plasma waves by the accelerated electrons. Estimates of the wave level and total energy in electrons that is required to produce the observed radio fluxes are obtained in the Appendix. Herringbone structure, band splitting, and other features of type II emission are discussed in § IV.

II. SHOCK DRIFT ACCELERATION

Drift acceleration occurs when a suprathermal charged particle is incident upon a nonparallel ($\boldsymbol{B}_1 \cdot \hat{n} \neq 1$; see Fig. 1), fast-mode MHD shock wave. As seen by an observer moving with a magnetosonic fast-mode shock, the upstream plasma enters the shock front at a speed greater than the fast-mode magnetosonic wave speed, while plasma leaves the shock front at a speed less than the fast-mode wave speed. The flow speed on either side of the shock exceeds the local Alfvén speed. When an energetic (kinetic energy > mean thermal energy; see Scott and Pesses 1982) charged particle is incident upon the shock, it will undergo a gradient B drift in the plane of the shock because of the increase in magnetic field strength across the shock front. As viewed in the rest frame of the shock front, there is a $\vec{v}_s \times \boldsymbol{B}$ electric field in the plane of the shock, where $\vec{v}_s$ is the shock velocity relative to the upstream plasma (cf. Fig. 1). This electric field in a fast-mode shock is parallel to the $\nabla \boldsymbol{B}$ drift motion of a proton and antiparallel to that of an electron and, hence, both particles are accelerated. The shock drift mechanism was first discussed for the case of oblique shock geometries by Sarris and van Allen (1974) and by Chen and Armstrong (1975). The shock drift mechanism is discussed in reviews by Armstrong *et al.*

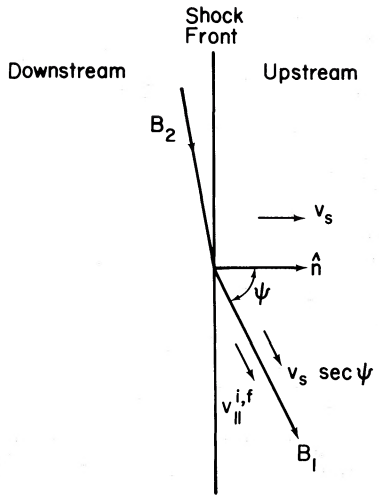

FIG. 1.—The shock geometry as observed in the rest frame of the upstream plasma is shown. The speed of propagation of the shock front is v_s, $B_1(B_2)$ is the upstream (downstream) magnetic field strength, $\hat{n}$ is the normal to the plane of the shock, and $v_{\parallel}^{i}(v_{\parallel}^{f})$ is the component of a particle's velocity parallel to the upstream magnetic field before (after) encountering and being reflected by the shock front.

(1977), Toptyghin (1980), Axford (1981), Pesses, Decker, and Armstrong (1982), and Pesses (1982).

The scale lengths involved in the drift acceleration of electrons and protons are quite different, because the suprathermal proton's gyroradius is comparable to or larger than the shock thickness while the electron gyroradius is generally much smaller than the shock thickness. The proton effectively encounters a discontinuous change in the magnetic field at the shock front while the electron encounters a continuous variation in B. Since the electron's magnetic moment is conserved while the proton's is not, one would not necessarily expect an encounter with the shock to have the same effect upon an electron as upon an ion. Numerical studies have shown, however, that when averaged over gyrophase for an initially gyrotropic distribution of ions, the preshock and postshock values of the magnetic moment are approximately equal for both reflected and transmitted ions (Pesses 1979; see also Pesses 1981 for a theoretical interpretation of this result). Hence, the effect of an encounter with the shock can be treated in the same manner for electrons as for ions.

A concern for shock drift acceleration is that wave turbulence associated with the shock wave will scatter the nonthermal particles and, therefore, inhibit the acceleration process. The effect of such waves upon the shock drift mechanism has been studied by Armstrong *et al.* (1977), who introduced random small-angle scattering into their numerical simulation of the particle trajectories. They found that the spectrum of energy

change of the particles in broadened, but the mean energy gain of the particles is not significantly affected.

With the requirement that a particle's (gyrophase averaged) pre- and post-encounter magnetic moments be equal, analytic expressions can be obtained for a particle's post-shock-encounter speed and pitch angle (Pesses 1979; Toptyghin 1980; Pesses, Decker, and Armstrong 1982). These results are most easily obtained by transforming to a reference frame in which the $\boldsymbol{v}_s \times \boldsymbol{B}$ electric field vanishes and, hence, the particle's energy remains unchanged. The post-encounter speed and pitch angle are then obtained by transforming back to the rest frame of the upstream plasma. For a reflected particle (of primary interest here) the velocity component perpendicular to the upstream magnetic field is unaffected (as is required for conservation of its magnetic moment), and its postencounter velocity is simply

$$v_{\parallel}^{f} = 2v_s \sec\psi - v_{\parallel}^{i} \tag{1}$$

where $v_{\parallel}^{i}$ ($v_{\parallel}^{f}$) is the particle's velocity component in the rest frame of the upstream plasma parallel to the upstream magnetic field before (after) the shock encounter and ψ is the angle between the shock normal ($\hat{n}$) and the upstream magnetic field (see Fig. 1). The parallel velocities $v_{\parallel}^{i}$ and $v_{\parallel}^{f}$ are taken to be positive when the particle is streaming away from the shock front (when observed in the frame of the upstream plasma). Equation (1) is valid for nonrelativistic velocities. We have assumed that v_s is parallel to the shock normal. When this is not the case, v_s should be replaced in equation (1) with $\boldsymbol{v}_s \cdot \hat{n}$. The energy gained by a particle is seen to increase with the shock speed (v_s) and with the obliquity of the shock (ψ). The energy gained by a particle is not unbounded as ψ goes to 90°, as indicated by equation (1), since particles are reflected only if

$$\sec\psi < (B_2/B_1)^{1/2}(v^{i}/v_s), \tag{2}$$

where $B_1(B_2)$ is the upstream (downstream) magnetic field strength (Pesses 1979). The condition $\sec\psi < c/v_s$ must also be satisfied for particles to be reflected.

An important signature of shock drift acceleration is the pitch angle distribution of reflected and transmitted particles in front of and behind the shock front (Sarris and van Allen 1974). Since reflected particles gain energy only in the component of their velocity parallel to the upstream magnetic field, an anisotropic, field-aligned flow of particles streaming away from the shock develops. Particles transmitted downstream gain most of their energy in the perpendicular component of their velocity so that their (average) magnetic moment is conserved. Hence, their pitch angle distribution is anisotropic and peaked at a high pitch angle to the downstream magnetic field. Such upstream and downstream distributions are commonly observed for protons accelerated by interplanetary shock waves (Pesses, Decker, and Armstrong 1982 and references therein) and have recently been observed for electrons as well (Potter 1981).

It should be noted that in addition to shock drift acceleration, particles can also be shock accelerated by being "compressed" between magnetic field irregularities upstream and downstream of the shock front (see Achterberg and Norman 1980 and references therein). This compression (Fermi acceleration) mechanism depends upon the particles being efficiently scattered in pitch angle both upstream and downstream of the shock. Since drift acceleration will occur with each encounter a particle makes with the shock front, particle acceleration will in general result from a combination of the shock drift and compression mechanisms. Particle energies will be further increased by multiple encounters with the shock front. As stated above, the energetic electron and ion distributions observed in the vicinity of interplanetary shock waves are characteristic of the shock drift acceleration mechanism. Hence, in this paper we concentrate upon determining how the simple shock drift acceleration of electrons can lead to type II radio emission.

As was stated above, the shock drift acceleration mechanism requires a population of particles which is already suprathermal. These particles may be produced by the associated flare ("first phase" acceleration), but they may also be picked up from the tail of the thermal coronal plasma. Scott and Pesses (1982) find that the shock drift acceleration mechanism will accelerate particles from the thermal electron distribution, with a larger fraction of the thermal electrons being picked up in higher β plasmas ($\beta \equiv 8\pi n_e k_B T_e/B^2$). The acceleration of thermal electrons is not very efficient in the solar corona, since $\beta \lesssim 0.1$. Our estimate in the Appendix of the number of accelerated electrons required to produce the observed type II emission indicates, however, that the acceleration need not be efficient. Our results and those of Scott and Pesses indicate that the accelerated particles may be picked up directly from the tail of the thermal electron distribution.

Thermal electrons may also be accelerated through the combined efforts of the shock drift and compression acceleration mechanisms. The direction of the upstream magnetic field (ψ) is likely to fluctuate as the shock propagates through the corona. The parallel speed gained by a particle in an encounter with the shock from shock drift acceleration is $\sim 2v_s \sec\psi$ (eq. [1]), while the gain per encounter from Fermi acceleration alone is $\sim 2v_s \cos\psi$. Hence, when the shock is quasi-parallel ($\psi \sim 0°$), the compression-Fermi acceleration mechanism (or the damping of downstream wave turbulence) can accelerate particles out of the thermal electron distribution (cf. Eichler 1979). When the shock is quasi-perpendicular ($\psi \sim 90°$), the particles will be efficiently

accelerated to higher energies by shock drift acceleration.

III. TYPE II EMISSION

We saw in the preceding section that shock drift acceleration results in an anisotropic, field-aligned flow of suprathermal electrons upstream of the shock front. Such a distribution is well known to be unstable to the emission of electrostatic plasma waves if the parallel velocity distribution (F) contains a region of positive slope (i.e., if $\delta F/\delta v_{\parallel} > 0$; cf. Krall and Trivelpiece 1973). This region of positive slope must be well above the electron thermal speed so that Landau damping does not prevent the growth of waves, implying that in the $\sim 2\times10^6$ K coronal plasma electron energies on the order of 200 eV or greater are needed. The initial electron velocity, v^i, must also be suprathermal so that the electron is accelerated and not treated as part of the thermal distribution (see Scott and Pesses 1982 for further analysis of this point). Hence we must have both v^i and $v_{\parallel}^f \gtrsim 8\times10^8$ cm s^{-1}.

As is noted by Ramaty *et al.* (1980), a sufficiently unstable distribution may result from the faster accelerated electrons (higher $v_{\parallel}^f$) outrunning the slower particles. The shock acceleration itself will produce the required region of positive slope, however, since only those electrons for which

$$v_{\parallel}^f > v_s \sec\psi \tag{3}$$

can outrun the advancing shock front (equivalently, $v_{\parallel}^i$ must be less than $v_s \sec\psi$ if the particle is to interact with the shock; see Fig. 1 and eq. [1]). Suprathermal electrons for which $0 < v_{\parallel}^i < v_s \sec\psi$ are accelerated to parallel velocities in the range $v_s \sec\psi < v_{\parallel}^f < 2vs \sec\psi$ (eq. [1]), with the lower velocity ($v_{\parallel}^i$) particles gaining the most parallel energy. For a typical monotonically decreasing velocity distribution, an unstable distribution will result in the region $v_{\parallel}^f \geq v_s \sec\psi$, below the velocity $v_{\parallel}^f = 2v_s \sec\psi$. Taking the shock speed to be 1000 km s^{-1} (2000 km s^{-1}), this unstable region will be above the thermal electron distribution if the shock normal has an inclination of $\psi \approx 80°$ (70°) or greater to the upstream magnetic field.

In § II we pointed out that particles are not reflected by the shock when ψ is near 90° (eq. [2]). For $B_2/B_1 = 3$, $v^i = 10^9$ cm s^{-1}, and $v_s = 1000$ km s^{-1} (2000 km s^{-1}), we find from eq. (2) that electrons are not reflected when $\psi > 86.^{\circ}7$ (83.°4). Hence, for a 1000 km s^{-1} shock, the production of type II emission requires $80° \lesssim \psi \lesssim 87°$.

Note that the typical electron velocity which is required for the production of herringbone structure (discussed in § IV) is on the order of 10^{10} cm s^{-1}. It can be seen from equations (1) and (2), however, that electrons of this velocity cannot be produced from a single encounter with the shock front unless $v^i \gtrsim 2\times10^9$ cm s^{-1} (~ 2 keV). Therefore, if the initial electron velocity is not greater than a couple of keV, more than one encounter with the shock front is required to produce the herringbone electrons.

The intensity of the radio emission at the plasma frequency (ω_e) and $2\omega_e$ depends upon the subsequent evolution of the coupled plasma wave and streaming electron distributions (cf. Melrose 1980). The emission at ω_e can be produced by the interaction of the plasma waves with density fluctuations in the (upstream) coronal plasma. Emission at $2\omega_e$ requires the presence of plasma waves propagating in opposite directions along the ambient magnetic field (the initially destabilized waves propagate in the same direction as the streaming electrons). The physical conditions encountered by upstream type II electrons are essentially the same as those encountered by type III radio burst electrons, the only difference being that the type II electron velocities can be lower than that of the streaming electrons responsible for type III bursts ($\sim c/3$). Since the question of how the electron and wave distributions evolve is still not settled and the physics is not fully developed, it is presently not possible to do a meaningful computation of the intensity of the type II emission. Using presently available theories for type III emission, however, it is possible to estimate the wave level required to produce the observed radio emission at $2\omega_e$ and to obtain an estimate of the minimum suprathermal electron density required to produce this wave level. These results are obtained in the Appendix.

IV. DISCUSSION

In addition to the direct observations of streaming, suprathermal electrons upstream of interplanetary shock fronts, there are several lines of evidence which indicate that type II emission is associated with shock-accelerated electrons which are streaming away from the shock front through the upstream plasma. The production of fast streams of electrons immediately upstream of a shock which produces a type II event is clearly indicated by the observations of type III bursts emanating from a type II backbone (Sheridan, Trent, and Wild 1959). Observations also indicate that when a type II burst follows a type III burst through the same region of the corona, the emission at a given frequency (and harmonic) originates from the same height in the corona for both bursts (Dulk, Altschuler, and Smerd 1971). This suggests that the type II emission is produced in the upstream coronal plasma rather than in the denser downstream plasma.

Since the type II bursts appear to follow the same open magnetic field lines which are required for the type III events, Dulk *et al.* interpret their results to imply that the type II shocks must be parallel or nearly parallel (i.e., $\psi \sim 0°$). We note here, however, that it is also likely

that other field orientations are present in the vicinity of the open field lines. The spatial resolution of the radio maps is not sufficient to determine whether the type II emission is produced along the same field lines followed by the type III bursts or along nearby field lines with a different orientation. We also note that a planar shock front propagating obliquely across these field lines, producing type II emission when it crosses this region (where $\psi \gtrsim 80°$ for a 1000 km s^{-1} shock so that the required plasma waves are produced), will produce a type II burst which follows the path of the preceding type III events. Hence, while the results of Dulk *et al.* do suggest that type II emission is generated in the upstream plasma, we do not feel that they supply substantial support for low values of ψ.

An important feature of type II emission is the herringbone structure observed in approximately 20% of the type II events (cf. Kundu 1965). These structures are similar to type III bursts in that they indicate the presence of fast streams of electrons with velocities which are typically on the order of 10^{10} cm s^{-1}. The particles are typically observed to propagate both upward and downward in the corona, to both lower and higher plasma densities. This feature can be understood to result from a curved shock front propagating across radial magnetic field lines, such as in a coronal streamer. Electrons accelerated and reflected by the shock are then free to stream both upward and downward through the corona, producing the herringbone structure (see Fig. 2*c*). This interpretation is supported by the unusually slow drift rate (in radio frequency) and large transverse motion of type II bursts containing herringbone structure (Weiss 1963; Stewart and Magun 1980). This type of picture is further supported by the recent observations at kilometric wavelengths of type III–like bursts in association with meter wavelength type II bursts having herringbone structure ("SA events"; Cane *et al.* 1981).

Herringbone emission is sometimes observed without the type II backbone (Kundu 1965). In §§ II and III we saw that particles are not reflected if ψ is within a few degrees of 90°. Hence, if the curvature of the shock front is sufficiently gradual, there will be two well separated particle acceleration regions and a significant region of space (and, therefore, coronal densities) between them over which reflected electrons are not present and plasma radiation is not produced (Fig. 2*d*). Under these conditions the type II backbone will not be observed.

The lack of reflected particles at the highest values of ψ may also be responsible for the band splitting which is sometimes observed in type II emission. Band splitting rather than herringbone structure without a backbone would be observed because the electrons in the unstable part of the upstream distribution have lower velocities and/or the upstream magnetic field has a larger angle to

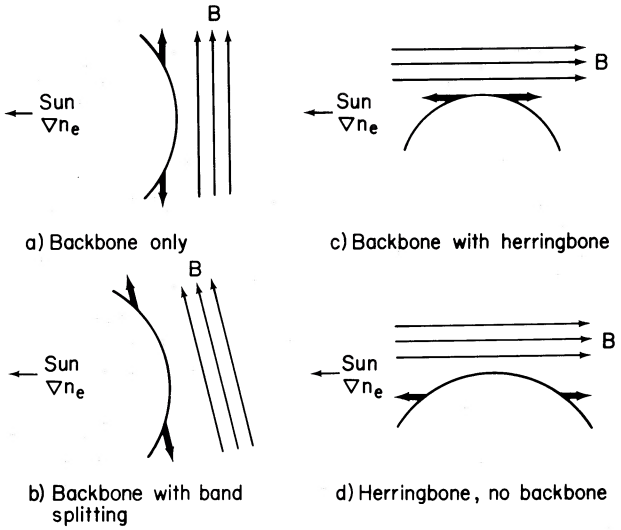

FIG. 2.—Examples of geometries in which band splitting, herringbone structure, and herringbone structure without a backbone will result are shown. The coronal plasma density (n_e) decreases from left to right in each figure. The curved line in each figure represents the shock front. The heavy arrows depict the regions where reflected electrons and plasma emission are produced. Note that, because of the influence of the coronal magnetic field, the density gradient may not always be radial as shown.

the coronal density gradient (Fig. 2*b*). (Band splitting could also result from a planar shock front moving nonradially across curved magnetic field lines, or a curved shock front with a spatially varying radius of curvature propagating across horizontal field lines.) The band splitting would only be observed if the frequency bandwidth of the splitting (as determined by the range of excluded coronal densities) is greater than the bandwidth of the emission at ω_e (or $2\omega_e$). A limiting case in which no band splitting is produced is illustrated in Figure 2*a*.

The explanation for band splitting presented here is similar to an earlier explanation by McLean (1967) in that the two bands originate from spatially distinct regions of the shock front. The spatial separation which is required to produce the observed band splitting can be estimated using a model for the coronal density distribution above an active region. Using Newkirk's (1961) density model, for a typical splitting of 18 MHz in the first harmonic emission at the 80 MHz level (Kundu 1965), a separation of approximately 0.1 $R_\odot$ ($\sim 1'.5$) is required. The separation will be larger when the coronal magnetic field is not parallel to the density gradient, as in Figure 2*b*. The observed separation is the projection of this distance onto the plane of the sky, however, and may therefore be smaller than the actual separation. Observations of split-band emission at a *single frequency* (the two bands are, therefore, seen at

different times) have in fact shown the emission from the two bands to originate from different locations. (See Smerd, Sheridan, and Stewart 1975 for references and further discussion of the observations. These authors interpret the two bands to arise from emission upstream and downstream of the shock front.)

A model of type II bursts involving the generation of the plasma emission by electrons streaming through the upstream coronal plasma has previously been published by Smith (1972). In his model, electrons are heated by ion acoustic turbulence behind the shock front, and fast electrons from the Maxwellian tail escape to the upstream region where they generate the required plasma waves. The angle between the shock normal and the upstream magnetic field must be within a few degrees of $\psi = 90°$ and the Alfvénic Mach number of the shock must be between approximately 2.0 and 2.9 for type II emission to be produced. On the other hand, for the shock drift acceleration model presented here, a less perpendicular shock is required, and electrons are not accelerated and reflected upstream when ψ is near 90°. There is also no restriction on the Mach number of the shock wave. A defect in Smith's model is that energy losses by the electrons as they traverse the electrostatic potential drop across the shock to the upstream region are not considered. Plasma turbulence such as that considered by Smith may, however, be a source of suprathermal seed particles for the shock drift mechanism.

In closing, we note that electrons accelerated and transmitted downstream of the shock wave may in some cases be responsible for the moving type IV emission which is associated with some type II bursts. As was discussed in § II, the particles downstream of the shock have a pitch angle distribution which is peaked at a high angle to the downstream magnetic field. When accelerated to energies on the order of 100 keV, these particles will be a good source of gyrosynchrotron radio emission, particularly in the enhanced magnetic field downstream of the shock. These particles may therefore be responsible for the continuum radio emission which is characteristic of moving type IV bursts.

The authors thank Drs. Tom Gergely, Mukul Kundu, Loukas Vlahos, and Donat Wentzel for their comments on the manuscript. We also thank the referee for several helpful comments. G. D. H. acknowledges partial support from NASA grants NGR 21-002-199, NGL 21-002-033, and NSG 5320. M. E. P. acknowledges support from the Laboratory for Astronomy and Solar Physics, NASA Goddard Space Flight Center, and from the National Academy of Science's National Research Council.

APPENDIX

We use the weak turbulence theory results of Smith (1977) to estimate the energy density of plasma waves which is required to produce the second harmonic type II emission. In Smith's (1977) theoretical model, backward moving plasma waves are produced by the induced scattering of the forward moving waves on thermal ion polarization clouds. He finds the volume emissivity at the second harmonic to be

$$J(2\omega_e) \approx 7\times 10^{-6} f(\mathrm{MHz})^3 \left(\frac{T_e}{2\times 10^6\ \mathrm{K}}\right)^2 \left(\frac{W}{n_e k_B T_e}\right)^2 \mathrm{ergs\ cm^{-3}\ s^{-1}\ sr^{-1}}, \quad \text{(A1)}$$

where f is the observation frequency is megahertz ($f = \omega_e/\pi$), T_e is the coronal electron temperature, W is the energy density in plasma waves, n_e is the thermal electron number density, and k_B is Boltzmann's constant. The volume emissivity is related to the observed radio flux, S, through the relation $J = R^2 S(\Delta f)/V$, where $R = 1$ AU, Δf is the bandwidth of the emission, and V is the emitting volume. The emitting volume is poorly known, since instrumental resolution is generally poor at metric wavelengths and refraction of the radio emission can give an apparent source size which is larger than the actual source size (cf. Kundu 1965). Observations at 80 MHz have yielded source sizes ~ 0.5 $R_\odot$. Hence we take $V \lesssim 3\times 10^{31}$ cm^3. For a representative value of the radio flux we take $S = 10^{-18}$ W m^{-2} Hz^{-1} at 80 MHz and $\Delta f = 20$ MHz, giving $J(2\omega_e) \gtrsim 2\times 10^{-13}$ ergs cm^{-3} s^{-1} sr^{-1}. Finally, from equation (A1) we obtain $(W/n_e k_B T_e) \gtrsim 2\times 10^{-7}$, or $W \gtrsim 2\times 10^{-9}$ ergs cm^{-3}.

Taking n_b to be the number density of the unstable, suprathermal electrons and v_b their mean streaming speed, the energy density in the streaming particles is approximately $(1/2) m_e n_b v_b^2$. How much of this energy goes into plasma waves depends, once again, upon the evolution of the coupled system of streaming electrons and plasma waves. If the system quasilinearly relaxes, the energy density in waves can build up to the level

$$W^{\mathrm{QL}} \approx \left(\frac{1}{15}\right) m_e n_b v_b^2 (v_b/v_e)^2 \quad \text{(A2)}$$

(Vedenov and Ryutov 1976; this quantity can be larger than the energy density in electrons because the low group velocity of the plasma waves allows them to pile up along the electron beam). This is the maximum wave energy density that can be obtained. If propagation effects (Magelssen and Smith 1977) or the transfer of waves to nonresonant wave numbers prevent quasi-linear relaxation, a higher particle density (or streaming velocity) will be required to produce a given level of wave turbulence. We can therefore estimate a lower limit on n_b by setting W^{QL} (eq. [A2]) equal to the wave level derived above ($W \gtrsim 2\times10^{-9}$ ergs cm^{-3}). With $v_b = 8\times10^8$ cm s^{-1} and $v_e = 5.5\times10^8$ cm s^{-1} ($T = 2\times10^6$ K), we obtain $n_b \gtrsim 20$ cm^{-3} ($n_b/n_e \gtrsim 10^{-6}$). A weaker (smaller) limit on n_b is obtained for higher values of v_b.

We note that weak turbulence theory is not valid if the wave level generated by the streaming electrons exceeds

$$W^{NL}/n_e k_B T_e \approx (k_1 \lambda_D)^2 \approx (v_e/v_b)^2, \tag{A3}$$

where k_1 is the wavenumber of the destabilized plasma waves and λ_D is the Debye wavelength (cf. Papadopoulos and Freund 1978). Under these circumstances the waves are expected to nonlinearly collapse to high (nonresonant) wave numbers. For $T = 2\times10^6$ K and $v_b = 8\times10^8$ cm s^{-1} (10^{10} cm s^{-1}), $W^{NL}/n_e k_B T_e \approx 0.5$ (3×10^{-3}). Our estimate of the wave level required to produce the second harmonic type II emission is much less than this and, therefore, nonlinear collapse is not indicated. Estimates of the required level of collapsed waves from Papadopoulos and Freund's (1978) result for the volume emissivity from close-packed solitons also yield a wave level which is much less than W^{NL}. If only a fraction of the observed source volume is filled with wave turbulence, however, so that a higher wave level is required, nonlinear collapse of the waves could be important.

For the assumed emission volume of $V \lesssim 3\times10^{31}$ cm^{-3}, the instantaneous number of required electrons is $N \sim 6\times10^{32}$, and the total energy in the accelerated ($v_b \approx 8\times10^8$ cm s^{-1}) particles is $E \sim 2\times10^{23}$ ergs. For a 20 minute radio burst with $v_s = 1000$ km s^{-1}, these numbers increase to $N \sim 1\times10^{34}$ electrons and $E \sim 3\times10^{24}$ ergs. For comparison, the total energy released in a typical flare which produces a type II event is on the order of 10^{30} ergs. Hence the energy in accelerated particles which is required to produce the type II emission is a small fraction of the total flare energy.

REFERENCES

Achterberg, A., and Norman, C. A. 1980, *Astr. Ap.*, **89**, 353.
Armstrong, T. P., Chen, E. T., Sarris, E. T., and Krimigis, S. M. 1977, in *Study of Travelling Interplanetary Phenomena/1977*, ed. M. A. Shea *et al.* (Dordrecht: Reidel), p. 367.
Axford, I. 1981, in *IAU Symposium 94, Origin of Cosmic Rays*, ed. G. Setti, G. Spada, and A. W. Wolfendale (Dordrecht: Reidel), p. 339.
Cane, H. V., Stone, R. G., Fainberg, J., Stewart, R. T., Steinberg, J. L., and Hoang, S. 1981, *Geophys. Res. Letters*, **8**, 1285.
Chen, G., and Armstrong, T. P. 1975, *Proc. 14th Int. Conf. Cosmic Rays*, **5**, 1814.
Dulk, G. A., Altschuler, M. D., and Smerd, S. F. 1971, *Ap. Letters*, **8**, 235.
Eichler, D. 1979, *Ap. J.*, **229**, 419.
Klinkhamer, F. R., and Kuijpers, J. 1981, *Astr. Ap.*, **100**, 291.
Krall, N. A., and Trivelpiece, A. W. 1973, *Principles of Plasma Physics* (New York: McGraw-Hill).
Kundu, M. R. 1965, *Solar Radio Astronomy* (New York: Interscience).
Magelssen, G. R., and Smith, D. F. 1977, *Solar Phys.*, **55**, 211.
McLean, D. J. 1967, *Proc. Astr. Soc. Australia*, **1**, 47.
_____. 1974, in *IAU Symposium 57, Coronal Disturbances*, ed. G. Newkirk (Dordrecht: Reidel), p. 301.
Melrose, D. B. 1980, *Plasma Astrophysics: Nonthermal Processes in Diffuse Magnetized Plasmas* (New York: Gordon & Breach).
Newkirk, G. 1961, *Ap. J.*, **133**, 983.
Papadopoulos, K., and Freund, H. P. 1978, *Geophys. Res. Letters*, **5**, 881.
Pesses, M. E. 1979, Ph.D. thesis, University of Iowa.
_____. 1981, *J. Geophys. Res.*, **86**, 150.
_____. 1982, *Adv. Space Res.*, **24**, in press.
Pesses, M. E., Decker, R. B., and Armstrong, T. P. 1982, *Space Sci. Rev.*, **32**, 185.
Potter, D. W. 1981, *J. Geophys. Res.*, **86**, 111.
Ramaty, R., *et al.* 1980, in *Solar Flares*, ed. P. Sturrock (Boulder: Colorado Associated University Press), p. 117.
Sarris, E. T., and van Allen, J. A. 1974, *J. Geophys. Res.*, **79**, 4157.
Scott, J. S., and Pesses, M. E. 1982, *J. Geophys. Res.*, submitted.
Sheridan, K. V., Trent, G. H., and Wild, J. P. 1959, *The Observatory*, **79**, 51.
Smerd, S. F., Sheridan, K. V. and Stewart, R. T. 1975, *Ap. Letters*, **16**, 23.
Smith, D. F. 1972, *Ap. J.*, **174**, 643.
_____. 1977, *Ap. J. (Letters)*, **216**, L53.
Stewart, R. T., and Magun, A. 1980, *Proc. Astr. Soc. Australia*, **4**, 53.
Toptyghin, I. N. 1980, *Space Sci. Rev.*, **26**, 157.
Vedenov, A. A. and Ryutov, D. D. 1976, *Rev. Plasma Phys. Consultants Bureau*), **6**, 1.
Weiss, A. A. 1963, *Australian J. Phys.*, **16**, 240.

GORDON D. HOLMAN: Astronomy Program, University of Maryland, College Park, MD 20742

M. E. PESSES: Code 602.6, Solar Activity Branch, Laboratory for Astronomy and Solar Physics, NASA Goddard Space Flight Center, Greenbelt, MD 20771